

# Neuroimaging in Pediatric Epilepsy: A Multimodality Approach<sup>1</sup>

Sachin Rastogi, MD • Christopher Lee, MD • Noriko Salamon, MD

## ONLINE-ONLY CME

See [www.rsna.org/education/rg\\_cme.html](http://www.rsna.org/education/rg_cme.html)

## LEARNING OBJECTIVES

After reading this article and taking the test, the reader will be able to:

- Discuss the role of multimodality imaging in pediatric epilepsy.
- Describe the importance of focal cortical dysplasias as a cause of intractable pediatric epilepsy.
- List the clinical and imaging findings of various pathologic conditions seen in patients with pediatric epilepsy.

## TEACHING POINTS

See last page

Pediatric patients with intractable epilepsy represent a challenging clinical population. However, recent advances in neuroimaging with a multimodality imaging approach that combines fluorine 18 fluorodeoxyglucose positron emission tomography, magnetoencephalography, diffusion tensor imaging, and magnetic source imaging with conventional magnetic resonance imaging continue to improve diagnosis and treatment in affected patients. These advances are increasing the understanding of the underlying disease process and improving the ability to noninvasively detect epileptogenic foci that in the past went undetected and whose accurate localization is crucial for a good outcome following surgical resection.

©RSNA, 2008 • [radiographics.rsnaajmls.org](http://radiographics.rsnaajmls.org)

**Abbreviations:** FCD = focal cortical dysplasia, FDG = fluorodeoxyglucose, FLAIR = fluid-attenuated inversion recovery, MCD = malformation of cortical development, MTS = mesial temporal sclerosis

RadioGraphics 2008; 28:1079–1095 • Published online 10.1148/rg.284075114 • Content Codes: **MR** **NM** **NR** **PD**

<sup>1</sup>From the Department of Radiological Sciences, David Geffen School of Medicine at UCLA, 10833 Le Conte Ave, Room BL-428/CHS, Los Angeles, CA 90095-1721. Presented as an education exhibit at the 2006 RSNA Annual Meeting. Received May 15, 2007; revision requested August 22 and received October 9; accepted October 22. All authors have no financial relationships to disclose. Address correspondence to N.S. (e-mail: [nsalamon@mednet.ucla.edu](mailto:nsalamon@mednet.ucla.edu)).

©RSNA, 2008

## Introduction

Each year approximately 30,000 new cases of pediatric epilepsy are reported (1). Approximately 25% of these cases are refractory to medical therapy, and patients are often severely debilitated by this disease (2). In patients with refractory epilepsy, neuroimaging is crucial for precisely identifying epileptogenic foci that are potentially amenable to surgical resection for possible cure. Some, but not all, causes of pediatric epilepsy are detectable with conventional magnetic resonance (MR) imaging. Advances in neuroimaging with use of diffusion tensor images, MR images fused with fluorine 18 fluorodeoxyglucose (FDG) positron emission tomographic (PET) images, and magnetic source images have recently improved lesion detection and localization. In this article, we review the latest imaging techniques in pediatric epilepsy and their capacity to help detect various pathologic entities, including focal cortical dysplasia (FCD), tuberous sclerosis, hemimegalencephaly, mesial temporal sclerosis (MTS), neoplasms, Rasmussen encephalitis, perinatal infarction, and Sturge-Weber syndrome.

## Imaging Techniques

A special consideration encountered in the imaging of pediatric epilepsy is the inability of children to cooperate for the long image acquisition times required. Motion artifact can significantly hinder the detection of subtle abnormalities associated with pediatric epilepsy. Ideally, this limitation is addressed with audio-video distraction, child-friendly surroundings, and, rarely, immobilization. However, in some cases sedation is required (3).

Routine MR imaging at our institution includes axial T1-weighted inversion recovery, T2-weighted, and fluid-attenuated inversion recovery (FLAIR) images; coronal magnetization-prepared rapid gradient-echo, T2-weighted, and FLAIR images; and sagittal T1-weighted images. All MR images are obtained at a 3-mm section thickness except magnetization-prepared rapid gradient-echo images, which are obtained at a 1.8-mm section thickness. In cases in which the epileptogenic substrate is not identified, further evaluation with diffusion tensor imaging, MR/FDG-PET fusion imaging, and magnetic source imaging is performed.

Diffusion tensor imaging is an MR imaging technique that makes use of the anisotropic diffusion of water to delineate microstructural tissue organization. It allows axonal fiber delineation, based on the observation that the diffusion of water in white matter is greater in directions

### Palmini Classification System for Cortical Dysplasias

Type of Cortical Dysplasia	Description
Mild MCD	
Type I	Ectopically placed neurons in or adjacent to cortical layer 1
Type II	Microscopic neuronal heterotopia outside cortical layer 1
FCD	
Type I	Architectural distortion of the cortical layer without dysmorphic neurons
Type IA	Isolated architectural abnormalities of the cortical layer
Type IB	Architectural abnormalities, giant or immature (but not dysmorphic) neurons
Type II	
Type IIA	Architectural distortion of the cortical layer with dysmorphic neurons but without balloon cells
Type IIB	Architectural distortion of the cortical layer with dysmorphic neurons and balloon cells

Source.—Reference 13.

parallel to fiber tracts but more limited in other directions. In diffusion tensor imaging, each voxel is color coded based on the most prominent direction of water diffusivity in the axial, sagittal, or coronal plane. Conventionally, blue is used for tracts in the superior-to-inferior direction, green for the anterior-to-posterior direction, and red for left to right. In addition, the data from diffusion tensor images can be displayed in a three-dimensional format referred to as fiber tractography. Diffusion tensor imaging has also been investigated in terms of its use in differentiating pathologic tissue from normal tissue based on differences in the anisotropic diffusion of water (4).

MR/FDG-PET fusion imaging is performed with software that registers MR images with FDG PET images. The two sets of images are obtained independently; however, patient positioning is similar to allow for coregistration of the images. This technique allows direct correlation of anatomic abnormalities detected at MR imaging with the metabolic abnormalities detected at FDG PET. In the interictal state, areas of abnormal activity are seen as foci of hypometabolic activity, whereas in the ictal state, they are seen as hypermetabolic foci (5,6). **Many subtle abnormalities that may go undetected at MR imaging are more readily appreciable with fusion imaging.**

Magnetic source imaging is derived from the coregistration of spatially localized data from a

Teaching  
Point

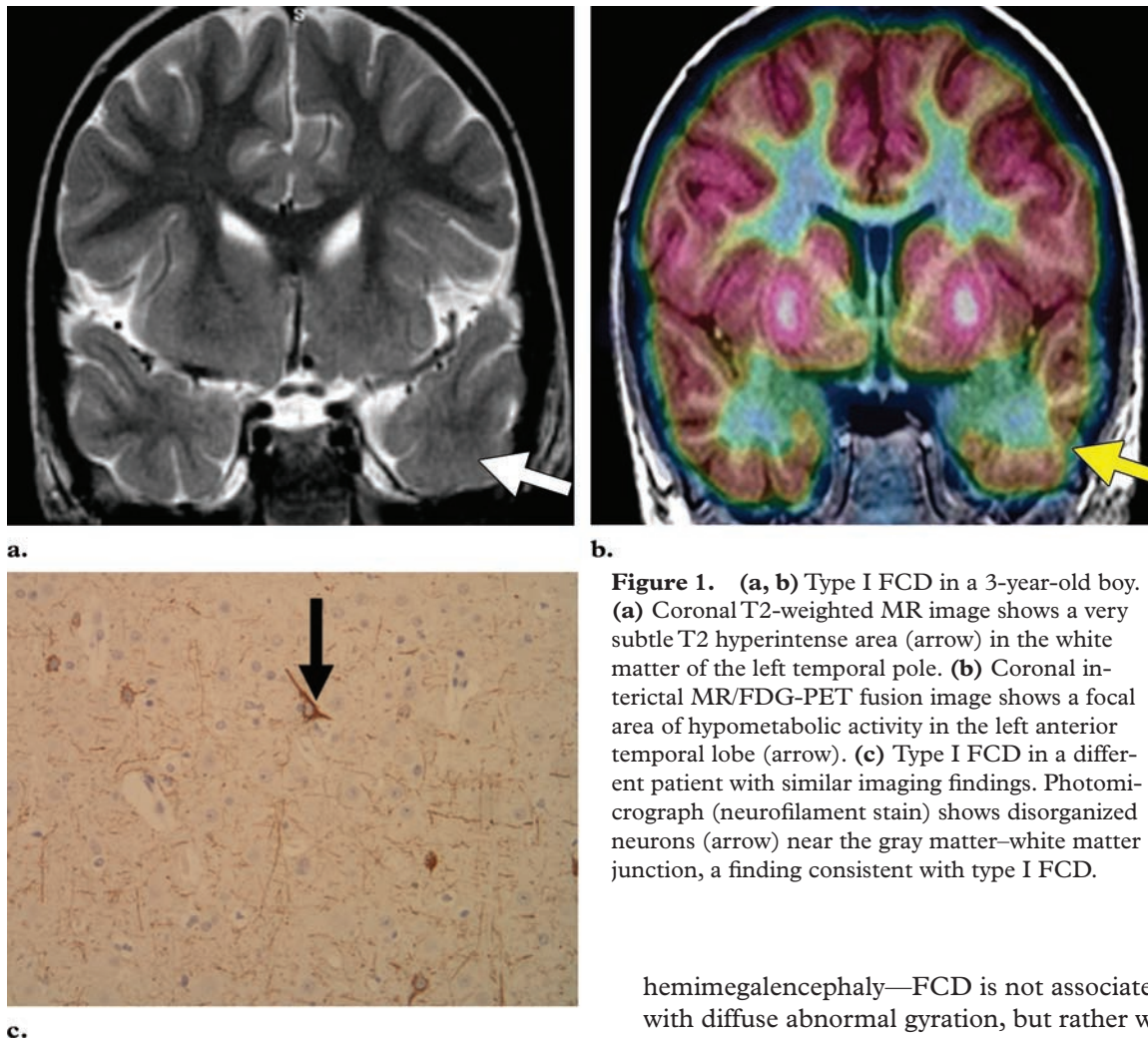


**Figure 1.** (a, b) Type I FCD in a 3-year-old boy. (a) Coronal T2-weighted MR image shows a very subtle T2 hyperintense area (arrow) in the white matter of the left temporal pole. (b) Coronal interictal MR/FDG-PET fusion image shows a focal area of hypometabolic activity in the left anterior temporal lobe (arrow). (c) Type I FCD in a different patient with similar imaging findings. Photomicrograph (neurofilament stain) shows disorganized neurons (arrow) near the gray matter–white matter junction, a finding consistent with type I FCD.

magnetoencephalogram with the anatomic data from MR imaging. This allows more precise localization of epileptogenic activity than that afforded by conventional electroencephalography. Unlike electroencephalography, magnetoencephalography helps detect the magnetic field produced by intracellular current flow in the active neurons instead of the distribution of extracellular volume currents. From the measured field, by making appropriate assumptions, it is possible to calculate the location of the activated brain area. With use of the anatomic data from MR imaging, the magnetoencephalographic data are coregistered to form magnetic source images (7). **Magnetic source imaging, like MR/FDG-PET fusion imaging, allows the detection of many subtle abnormalities that may otherwise go undetected with conventional MR imaging.**

### Focal Cortical Dysplasia

FCD was first described in 1971 by Taylor et al (8) as a distinct subtype of malformation of cortical development (MCD). Unlike other MCDs—which include pachygyria, polymicrogyria, and

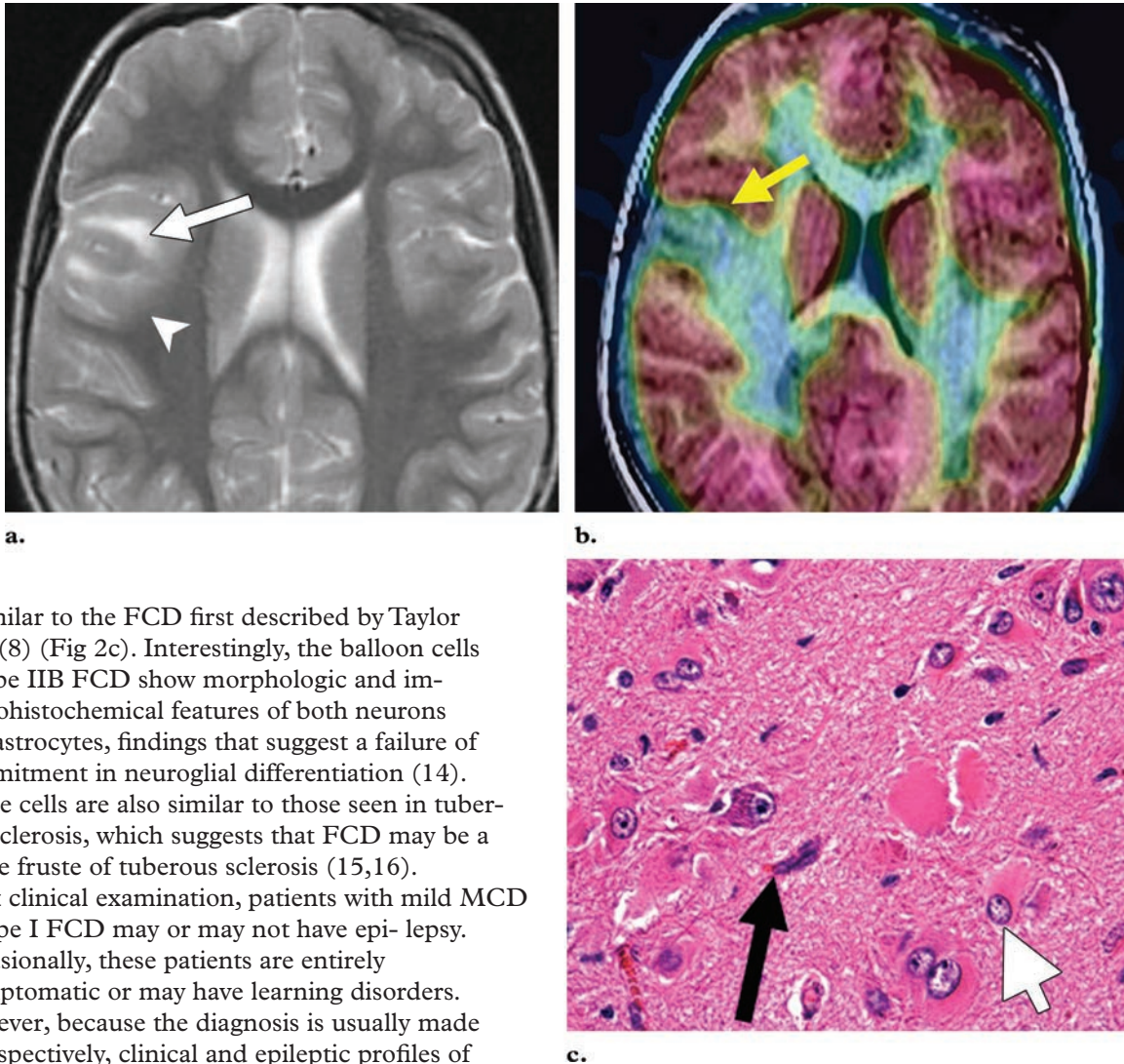
hemimegalencephaly—FCD is not associated with diffuse abnormal gyration, but rather with subtle focal changes that at times can only be appreciated microscopically (9). Similar to other MCDs, FCD is thought to be secondary to genetic, ischemic, toxic, or infectious insult during cortical development (10). Epilepsy associated with FCD is often highly refractory to medication because of the high intrinsic epileptogenicity of these lesions (11). **FCD is now recognized as one of the most common causes of seizures in children with intractable epilepsy, accounting for nearly 80% of all surgically treated cases in children under 3 years of age (12).**

Pathologic classification of cortical dysplasias is made according to the recently described method of Palmini et al (13). As shown in the Table, there are two major subdivisions of FCD. In type I FCD, there is dyslamination of the cortical layer compared with the normal cortex (Fig 1c). In type II FCD, along with cortical dyslamination, there are dysmorphic neurons. An additional finding of balloon cells associated with cortical dyslamination and dysmorphic neurons is more precisely classified as type IIB FCD and

Teaching  
Point

Teaching  
Point

**Figure 2.** (a, b) Type II FCD in a 3-year-old boy. (a) Axial T2-weighted MR image shows focal blurring of the gray matter–white matter junction (arrowhead) and abnormal T2 hyperintensity in the right inferior frontal gyrus opercular region (arrow). (b) Axial interictal MR/FDG-PET fusion image shows focal hypometabolic activity (arrow). Pathologic evaluation demonstrated type IIB FCD. (c) Type II FCD in a different patient. Photomicrograph (hematoxylin-eosin stain) shows dysmorphic neurons (black arrow) and balloon cells (white arrow) in the cortex, findings that are consistent with type IIB FCD.



is similar to the FCD first described by Taylor et al (8) (Fig 2c). Interestingly, the balloon cells in type IIB FCD show morphologic and immunohistochemical features of both neurons and astrocytes, findings that suggest a failure of commitment in neuroglial differentiation (14). These cells are also similar to those seen in tuberous sclerosis, which suggests that FCD may be a forme fruste of tuberous sclerosis (15,16).

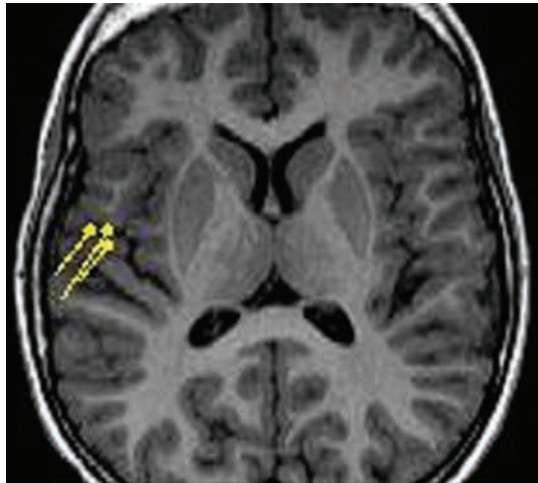
At clinical examination, patients with mild MCD or type I FCD may or may not have epilepsy. Occasionally, these patients are entirely asymptomatic or may have learning disorders. However, because the diagnosis is usually made retrospectively, clinical and epileptic profiles of these patients are not well established. Most patients with type II FCD have medically refractory epilepsy (13). **Regardless of the underlying disease, patients in whom the lesions are visualized at preoperative MR imaging tend to have a better outcome after surgery for epilepsy than do patients in whom the lesions are not delineated with MR imaging (17).**

Current imaging techniques that make use of MR imaging, magnetic source imaging, or FDG PET are unable to reliably help differentiate between mild MCD, type I FCD, and type

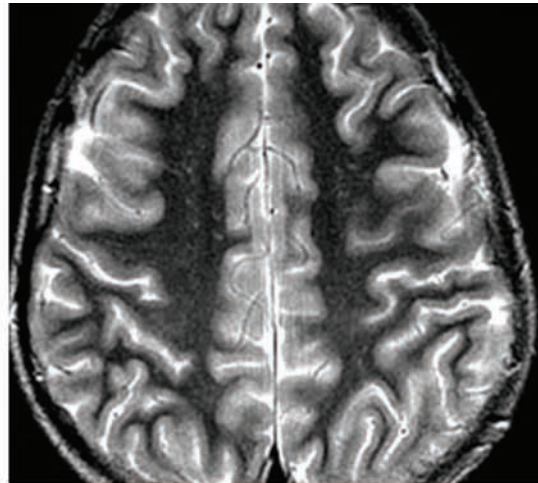
II FCD (Figs 1–6). However, the presence of subcortical T2 hyperintensity, especially when seen to extend to the ventricle, is most often associated with type IIB FCD (Fig 2) (13). This T2 hyperintensity is thought to be secondary to the degree of hypomyelination, rather than from balloon cells themselves (18). Other characteristic MR imaging findings of FCD include focal cortical thickening, blurring of the gray matter–white matter junction, and gray matter T2 hyperintensity (Fig 6). The findings of FCD can be subtle or undetectable at MR imaging alone (Figs 1, 3, 4). However, MR/FDG-PET fusion imaging and

#### Teaching Point

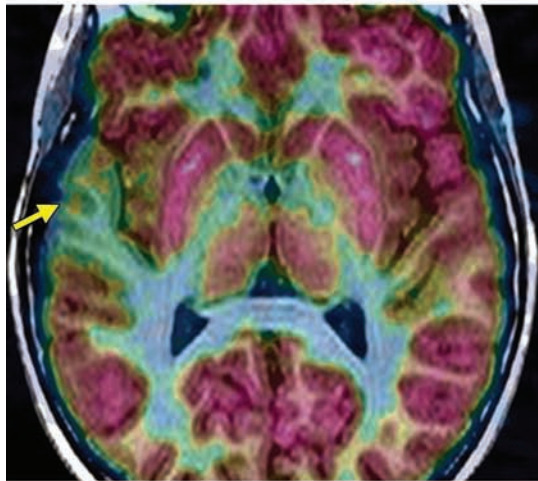
**Figures 3, 4.** (3) Type I FCD in an 8-year-old boy. (a) Axial magnetic source image shows epileptiform activity in the right anterior temporal lobe. (b) Axial interictal MR/FDG-PET fusion image demonstrates hypometabolic activity in the right anterior temporal lobe (arrow). (c) T2-weighted MR image shows subtle white matter T2 hyperintensity on the affected side (arrow) compared with the normal side (arrowhead), a finding that was appreciated retrospectively. Pathologic analysis demonstrated Palmini type IB FCD. (4) Type I FCD in a young child with intractable epilepsy. (a) Axial T2-weighted MR image shows no appreciable abnormality. (b) Axial T1-weighted magnetic source image shows epileptogenic foci in the right posterior parame-dian frontal lobe. (c) Photomicrograph (hematoxylin-eosin stain) shows ectopic neurons at the gray matter–white matter border (arrow) without evidence of dysmorphic neurons, findings that are consistent with type I FCD (confirmed at pathologic analysis).



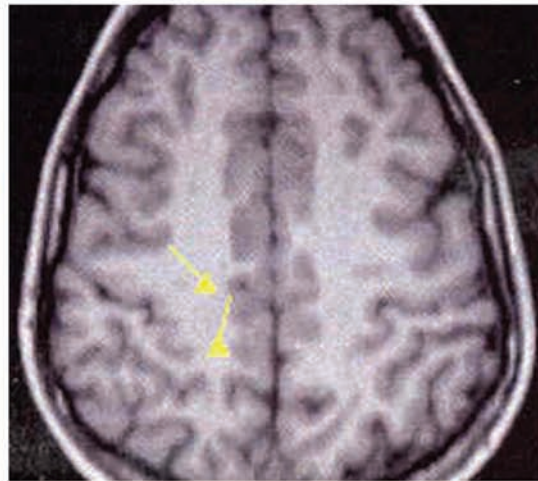
3a.



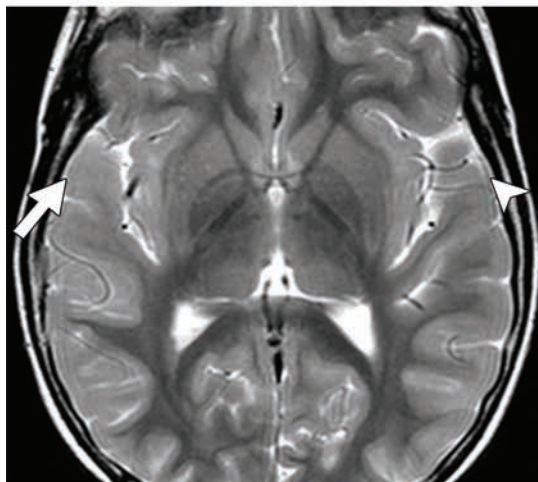
4a.



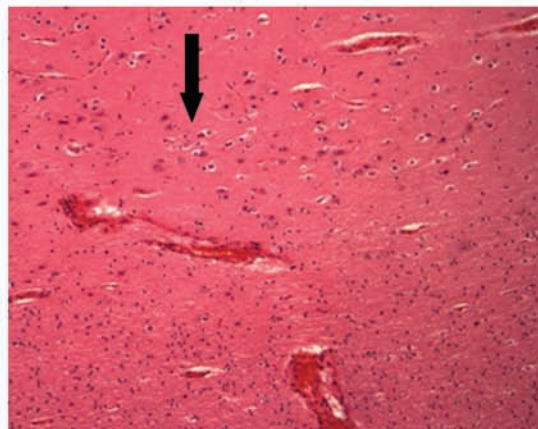
3b.



4b.



3c.



4c.

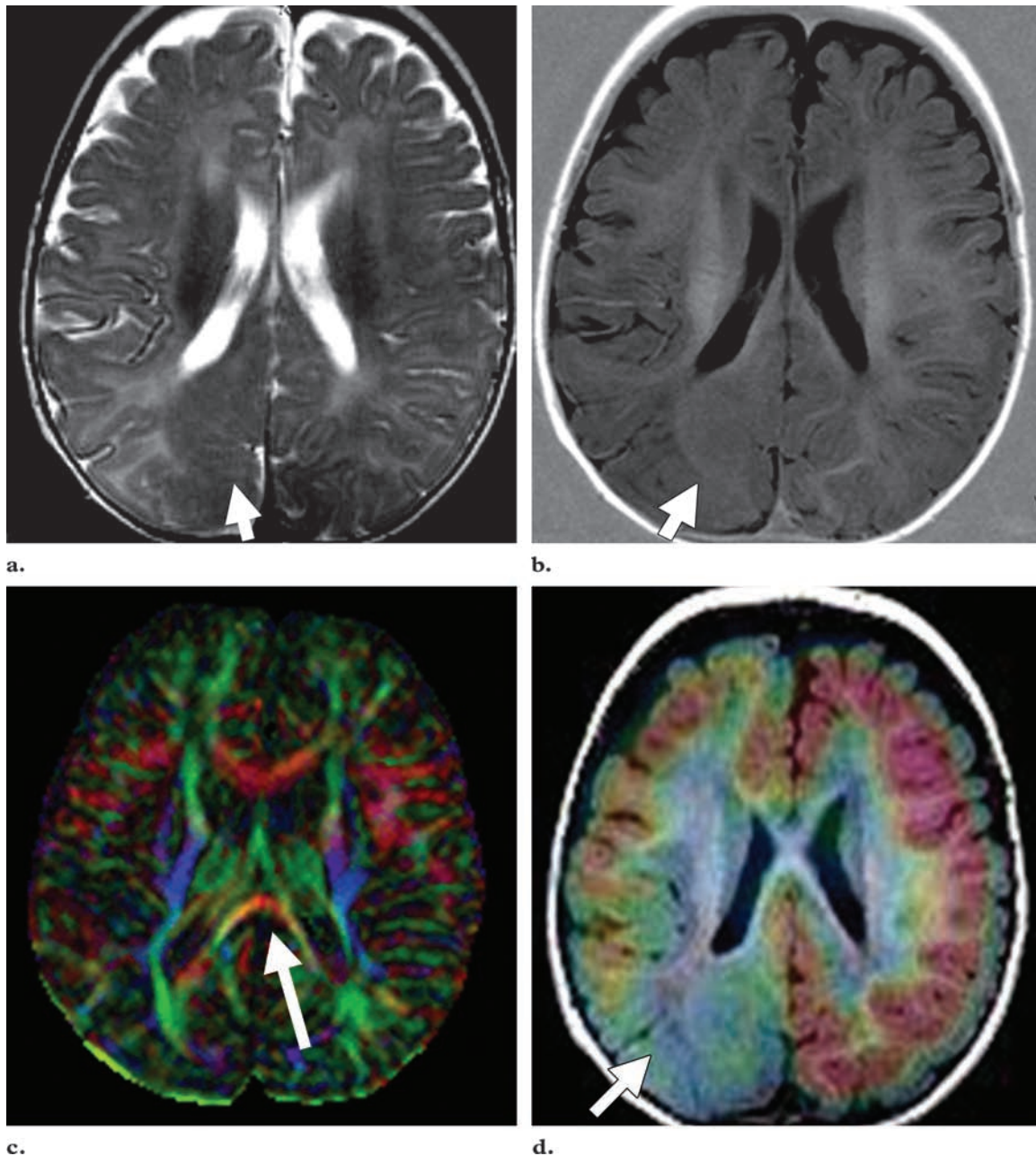


**Figure 5.** Type II FCD in a 10-month-old boy with congenital epilepsy. **(a)** Axial T2-weighted MR image shows focal cortical thickening of the gray matter in the right parietal region (arrow). **(b)** Axial T1-weighted MR image shows blurring of the gray matter–white matter junction (arrow). **(c)** Axial diffusion tensor image shows a thin splenium (arrow), a finding that suggests hypomyelination. **(d)** Interictal MR/FDG-PET fusion image shows a large area of hypometabolic activity (arrow). Pathologic evaluation revealed type IIA FCD.

magnetic source imaging can help localize subtle architectural and signal abnormalities seen at MR imaging. Interictal FDG PET demonstrates

areas of hypometabolic activity in regions of the cortex involved by FCD (Figs 1, 3–5). Interictal magnetic source imaging demonstrates areas of epileptiform spikes arising from the FCD (Figs 3a, 4b).

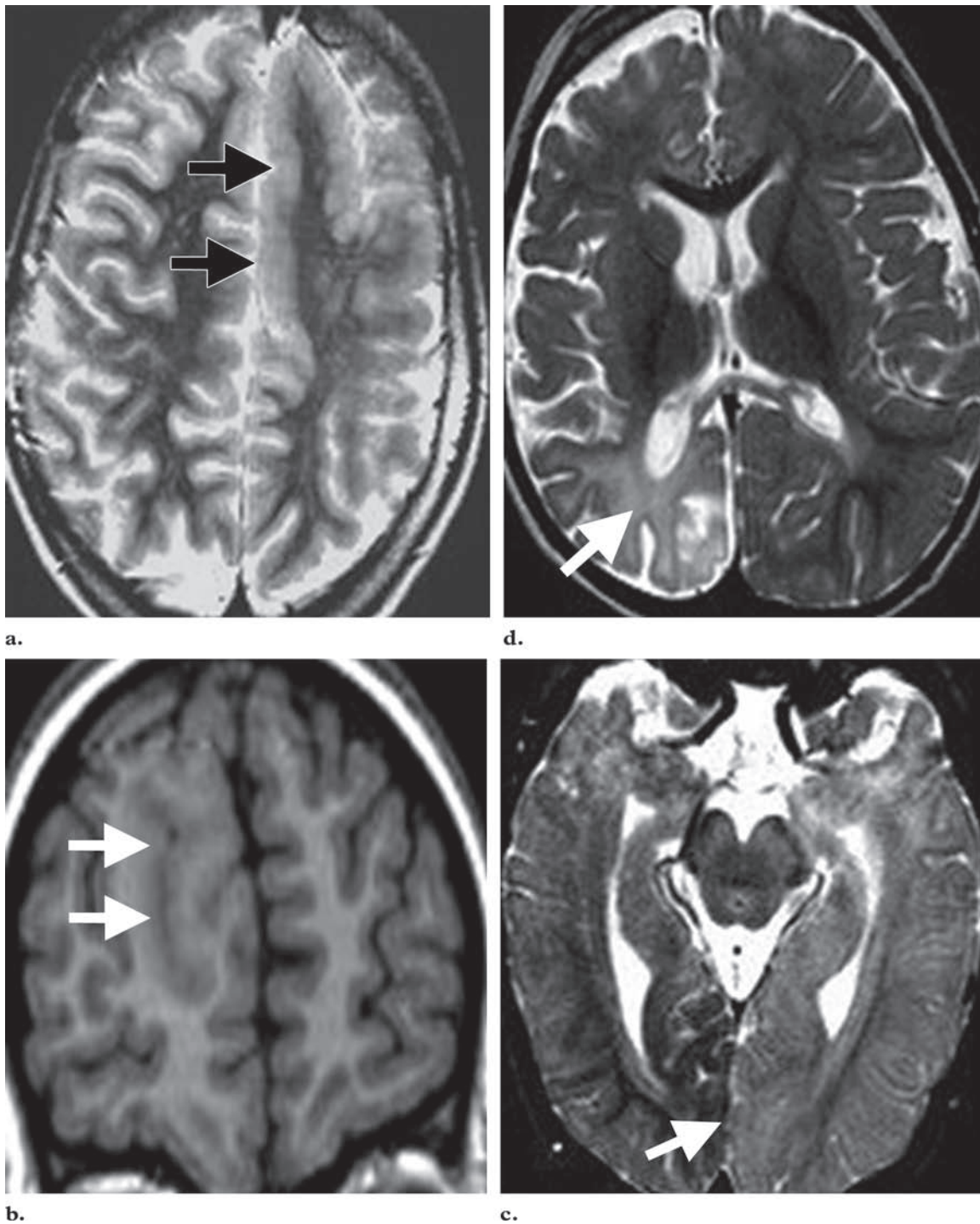


**Figure 6.** FCD. (a) Axial T2-weighted MR image shows thickening of the gray matter (arrows). (b) Coronal T1-weighted MR image shows blurring of the gray matter–white matter junction (arrows). (c, d) Axial T2-weighted MR images show hyperintensity of the gray matter (arrow in c) and white matter (arrow in d).

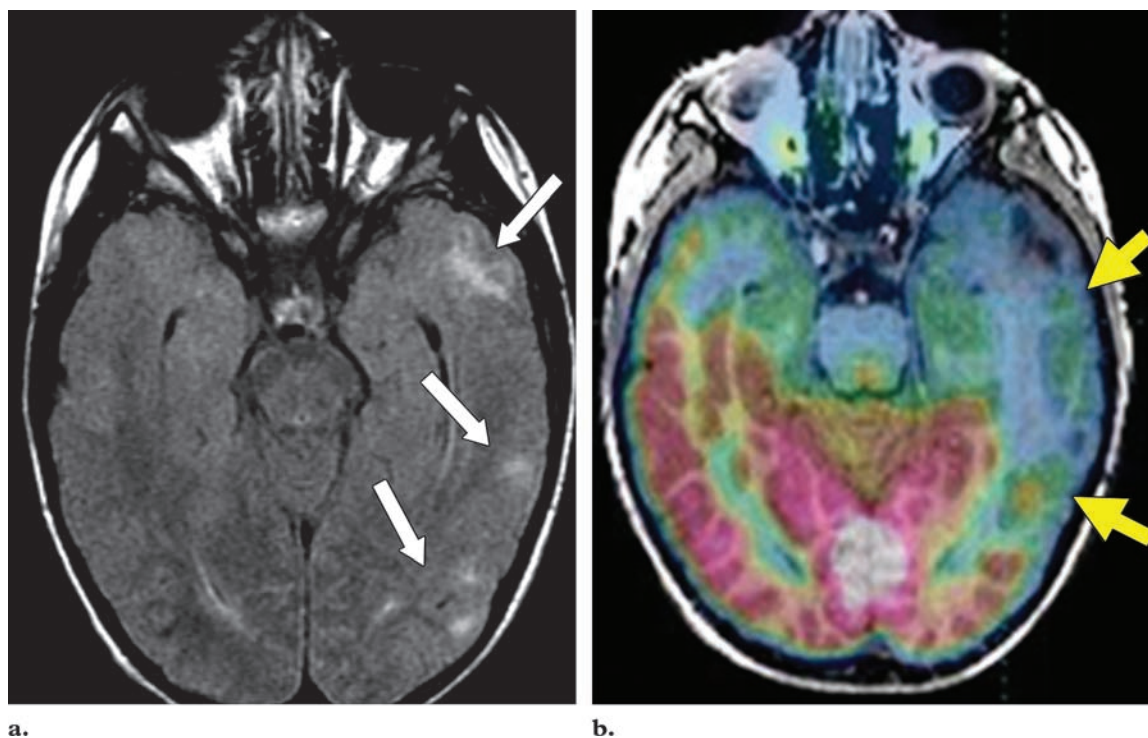


**Figure 7.** Tuberosclerosis and intractable epilepsy secondary to a left anterior temporal lobe tuber. **(a)** Axial FLAIR image shows multiple cortical and subcortical tubers (arrows). **(b)** Axial interictal MR/FDG-PET fusion image shows a large area of hypometabolic activity in the left temporal lobe (arrows). Intraoperative electrocorticography showed diffuse slowing in the hypometabolic region, a finding that suggests an epileptogenic zone.

### Tuberous Sclerosis

Tuberous sclerosis is an autosomal dominant disorder that results in multiorgan hamartomas. It has a prevalence of one in 6000–12,000 live births (19). At clinical examination, tuberous sclerosis is characterized by the triad of facial angiofibromas, mental retardation, and seizures (19). As many as 90% of patients with tuberous sclerosis have seizures (20), a significant proportion of whom are refractory to medical therapy (21). Central nervous system involvement by tuberous sclerosis is characterized by cortical tubers, subependymal nodules, and subependymal giant cell astrocytomas. Often, the ictal onset zone is related to a tuber and adjoining cerebral cortex. Cortical tubers are readily identified at MR imaging as areas of T1 and T2 signal abnormality that varies depending on the degree of myelination. In neonates, the tubers are seen as

regions of subcortical T1 hyperintensity and T2 hypointensity, but after about 6 months of age the signal intensity characteristics are reversed (22).

Tuberous sclerosis patients with medically refractory epilepsy usually have multiple tubers. Therefore, it is crucial to identify precisely which of the tubers are responsible for epileptogenic activity. This is not possible with MR imaging alone. By correlating the MR imaging data with electroencephalographic data, it is sometimes possible to localize the lesion (23). More recently, MR/FDG-PET fusion imaging and magnetic source imaging have shown promise in the improved localization of epileptogenic foci associated with tuberous sclerosis (5,24). **Interictal MR/FDG-PET fusion imaging demonstrates tubers with epileptogenic activity as regions of hypometabolic activity that are larger than the corresponding regions of signal abnormality (ie, T2 hyperintensity for patients older than 6 months) at MR imaging (Fig 7).** Interictal magnetic

**Teaching Point**

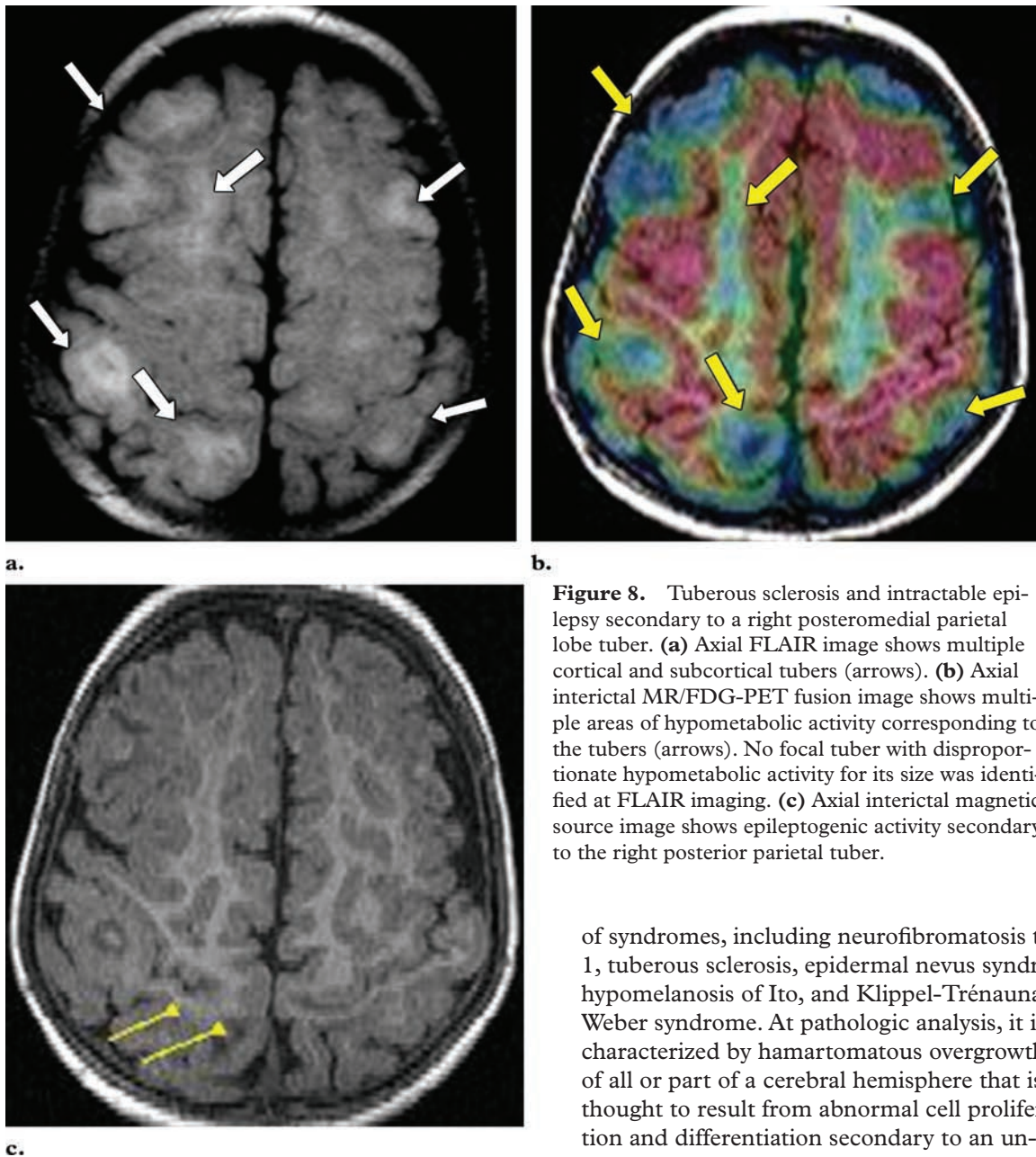


**Figure 8.** Tuberosclerosis and intractable epilepsy secondary to a right posteromedial parietal lobe tuber. **(a)** Axial FLAIR image shows multiple cortical and subcortical tubers (arrows). **(b)** Axial interictal MR/FDG-PET fusion image shows multiple areas of hypometabolic activity corresponding to the tubers (arrows). No focal tuber with disproportionate hypometabolic activity for its size was identified at FLAIR imaging. **(c)** Axial interictal magnetic source image shows epileptogenic activity secondary to the right posterior parietal tuber.

source imaging demonstrates areas of epileptogenic tubers by localizing the epileptiform spikes to their anatomic location on MR images (Fig 8).

### Hemimegalencephaly

Hemimegalencephaly is a severe, rare MCD that was first described in 1835 by Sims (25). It can occur on its own or in association with a variety

of syndromes, including neurofibromatosis type 1, tuberous sclerosis, epidermal nevus syndrome, hypomelanosis of Ito, and Klippel-Trénaunay-Weber syndrome. At pathologic analysis, it is characterized by hamartomatous overgrowth of all or part of a cerebral hemisphere that is thought to result from abnormal cell proliferation and differentiation secondary to an unknown cause. At clinical examination, it is usually dominated by severe and drug-resistant epilepsy. Other common findings include macrocrania, mental retardation, unilateral motor deficit, and hemianopia, findings that suggest that the grossly affected cortex is nonfunctional. Early hemispherectomy or hemispherotomy is the recommended surgical therapy (26).

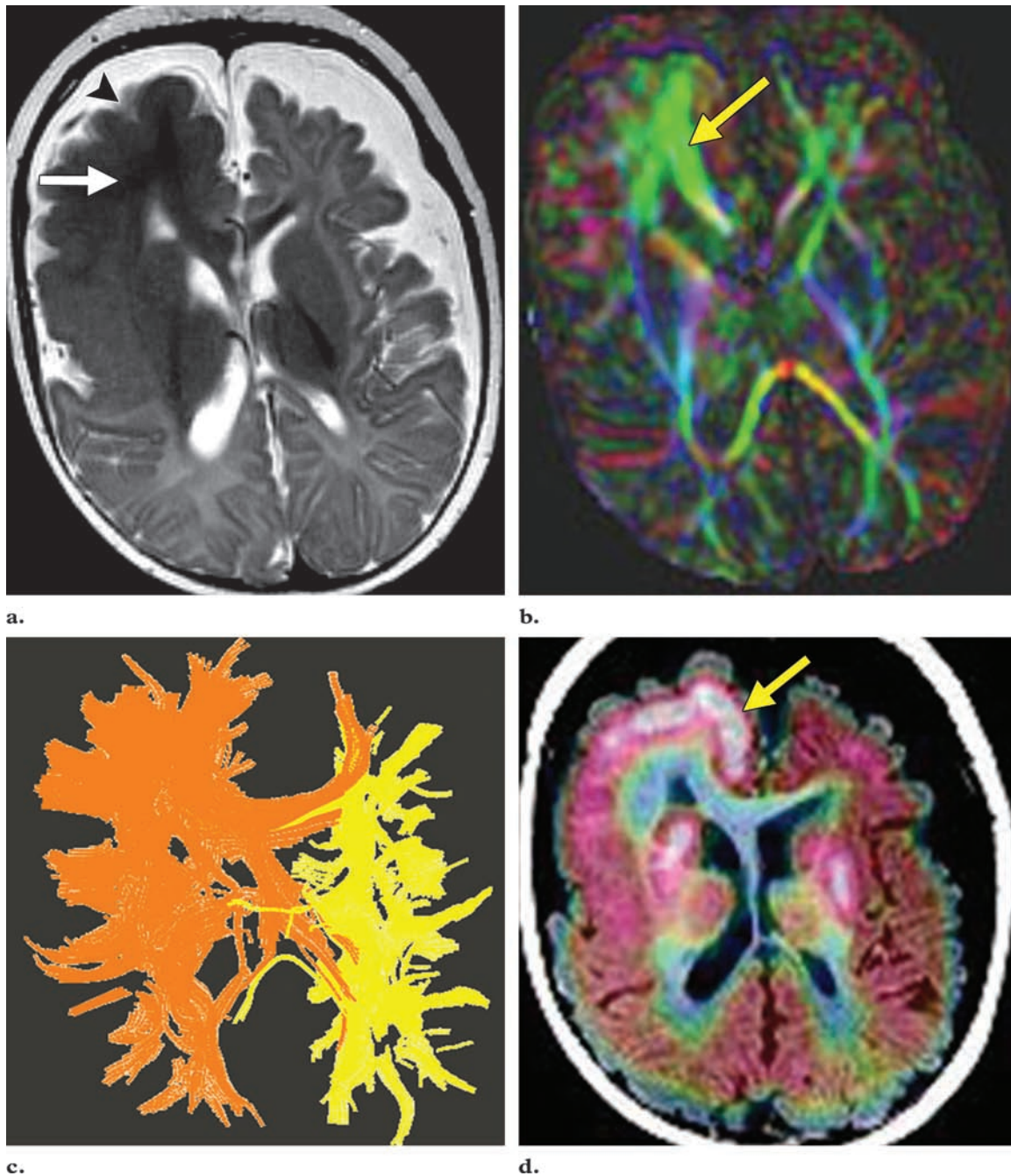


**Figure 9.** Right hemimegalencephaly in a patient with intractable epilepsy. **(a)** Axial T2-weighted MR image shows pachygyria and right cortical thickening (arrowhead) and abnormal T2 hypointensity of the subjacent white matter (arrow). **(b)** Axial diffusion tensor image shows hypermyelination in the white matter of the right anterior frontal lobe (arrow), a finding that accounts for the abnormal T2 hypointensity seen in **a**. **(c)** Tractograph shows more abundant fibers in the right hemisphere than on the normal left side. **(d)** Axial ictal MR/ FDG-PET fusion image shows an area of hypermetabolic activity (arrow) in the cortex of the right frontal lobe during a seizure.

Hemimegalencephaly has characteristic MR imaging features. The most notable characteristic is unilateral cortical thickening involving all or part of the cerebral hemisphere. The involved hemisphere also demonstrates ipsilateral white matter changes secondary to hypermyelination,

which is dependent on the underlying myelination state (27). Hamartomatous involvement of the ipsilateral basal ganglia and olfactory tract may also be present. In addition, ipsilateral enlargement of the lateral ventricle is often seen (Fig 9). Advanced neuroimaging techniques such as diffusion tensor imaging and MR/FDG-PET fusion imaging have also improved our under-

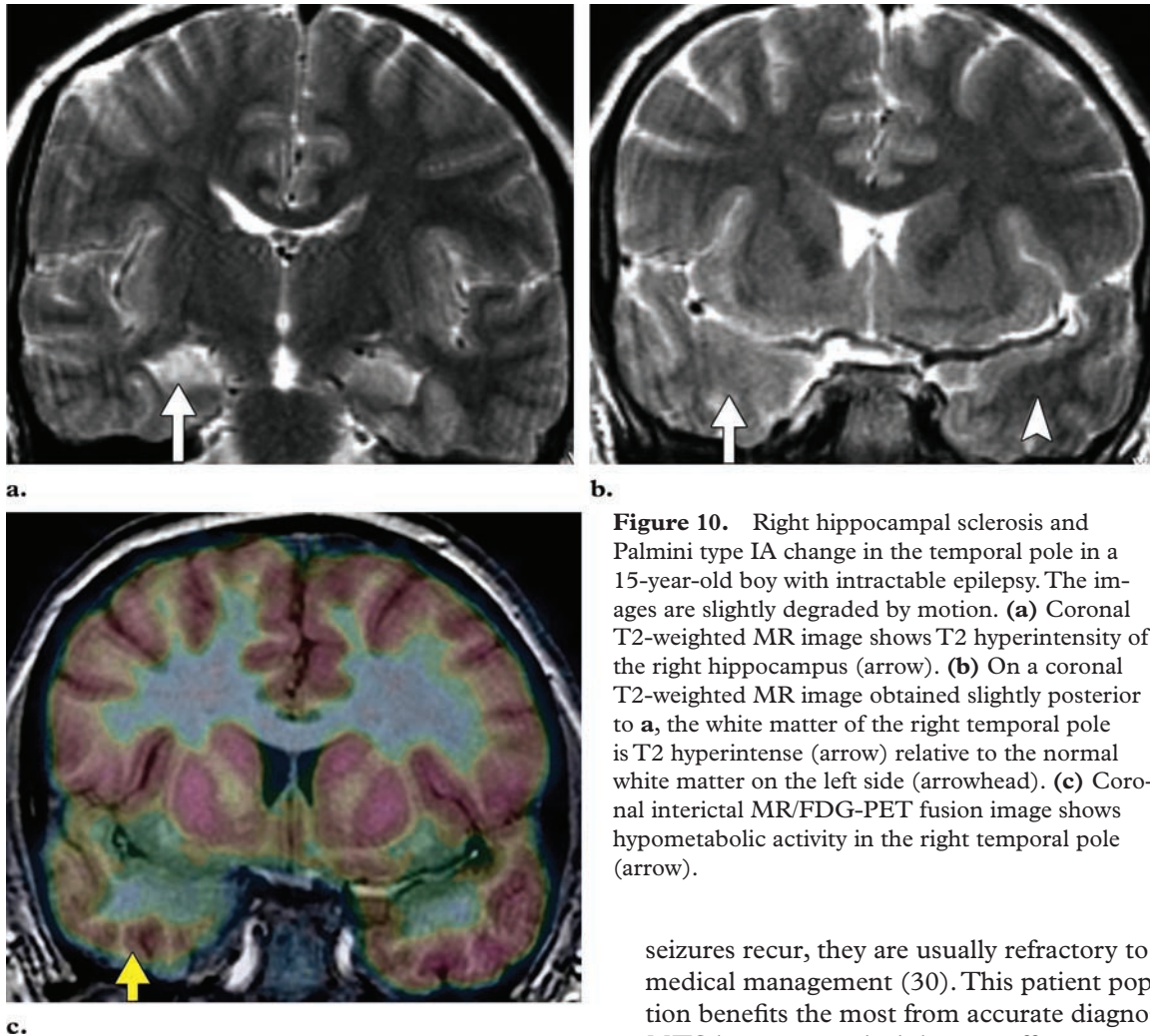


**Figure 10.** Right hippocampal sclerosis and Palmini type IA change in the temporal pole in a 15-year-old boy with intractable epilepsy. The images are slightly degraded by motion. **(a)** Coronal T2-weighted MR image shows T2 hyperintensity of the right hippocampus (arrow). **(b)** On a coronal T2-weighted MR image obtained slightly posterior to **a**, the white matter of the right temporal pole is T2 hyperintense (arrow) relative to the normal white matter on the left side (arrowhead). **(c)** Coronal interictal MR/FDG-PET fusion image shows hypometabolic activity in the right temporal pole (arrow).

standing of this disorder. Diffusion tensor imaging and fiber tractography suggest the presence of hypermyelination in the abnormal cerebral hemisphere as a region of asymmetrically increased anisotropic movement of water molecules (Fig 9b, 9c). Ictal MR/FDG-PET fusion images clearly demonstrate areas of asymmetric hypermetabolic activity in the involved cerebral cortex (Fig 9d).

### Mesial Temporal Sclerosis

MTS is one of the most common causes of epilepsy in the adolescent and young adult population. At pathologic analysis, it is characterized by neuronal loss with gliosis in the hippocampus and may also involve the ipsilateral fornix and mamillary body (28). At clinical examination, patients often have a history of a cortical insult such as intracerebral infection, head trauma, or complicated febrile seizures during the first 4–5 years of life (29). Medical management is usually sufficient initially, and patients may actually become seizure free without medication. When

seizures recur, they are usually refractory to medical management (30). This patient population benefits the most from accurate diagnosis of MTS because surgical therapy offers cure rates near 90% (31).

The diagnosis of MTS is based on concordance of clinical, electroencephalographic, and imaging data. Characteristic MR imaging features of MTS include atrophy of the hippocampus on T1-weighted images and increased signal intensity in the mesial temporal region on T2-weighted images (32,33). However, functional imaging with FDG PET is likely a more sensitive test for hippocampal sclerosis and usually shows an area of hypometabolic activity that is larger than just the hippocampus (34). This is especially true with the use of MR/FDG-PET fusion imaging (Fig 10).

### Neoplasms

Neoplasms of the central nervous system in pediatric patients often manifest clinically as seizures. Although any of these neoplasms may result in pediatric epilepsy, certain tumors are characteristically associated with this clinical manifestation. A group of these tumors sharing similar

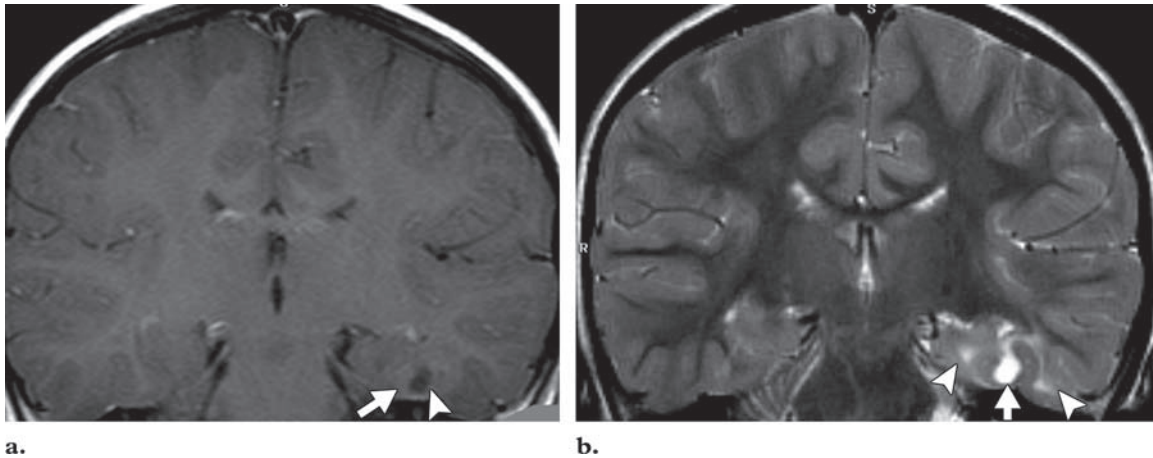


**Figure 11.** Left temporal lobe ganglioglioma and FCD. **(a)** Coronal contrast material–enhanced T1-weighted MR image shows a cortically based lesion in the left anterior temporal pole with a nonenhancing solid component (arrow) and a cystic component (arrowhead). **(b)** Coronal T2-weighted MR image shows areas of T2 hyperintensity (arrowheads) surrounding the lesion (arrow), findings that proved to be FCD associated with a ganglioglioma at pathologic analysis. Perilesional edema with ganglioglioma is rare.

clinical-pathologic features are referred to as epilepsy-associated developmental tumors and include ganglioglioma, gangliocytoma, desmoplastic infantile ganglioglioma, dysembryoplastic neuroepithelial tumor, and pleomorphic xanthoastrocytoma (35).

The epilepsy-associated developmental tumors all contain varying amounts of glial and neural elements. They are usually associated with benign behavior and a low proliferation index, and as such they are stable to slow growing over time, with good demarcation between normal and abnormal tissue and with minimal or no edema (36). A small percentage of these tumors may undergo malignant transformation (37). At clinical examination, they are most commonly seen in children and young adults. They may be seen in association with FCD. Some investigators have even postulated that FCD and these tumors may be derived from the same precursor cells and that the tumor may actually originate in the dysplastic tissue. Furthermore, the epileptogenicity of these developmental tumors may be related to dysplastic neurons as seen in FCD (35,38). These tumors have quite similar imaging features. At MR imaging, they usually appear as cortically based lesions that are hypo- to isointense on T1-weighted images and hyperintense on T2-weighted images. T2 hyperintensity does not necessarily reflect underlying cystic disease. Typically, little or no edema is present. Contrast material enhancement is common but may not

always be present (Fig 11) (37). Treatment consists of surgical resection (38).

Hypothalamic hamartoma is another neoplasm in the pediatric population. It is characteristically associated with gelastic seizures. Intrahypothalamic hamartomas, which extend toward the third ventricle, are associated with the early occurrence of epilepsy, whereas parahypothalamic hamartomas, which do not involve the third ventricle, are more closely associated with central precocious puberty. At MR imaging, these lesions are slightly hypointense on T1-weighted images and slightly hyperintense on T2-weighted images. Characteristically, there is no enhancement. Epileptogenic hamartomas always involve the mammillary bodies and, in 90% of patients, the tuber cinereum as well (39). The first-line treatment is medical therapy with hormonal suppressive therapy and antiepileptic medications. However, many cases become refractory to medical therapy and require surgical resection or radiosurgery (Fig 12) (35,40).

### Rasmussen Encephalitis

Rasmussen encephalitis is a rare childhood syndrome characterized by medically refractory focal seizures and progressive multifocal neurologic symptoms such as hemiplegia and cognitive impairment (41). Pathologic analysis demonstrates chronic progressive unilateral inflammation of the brain of uncertain cause that results in progressive cortical atrophy (42). At present, early functional or anatomic hemispherectomy is the recommended treatment for seizure control, thereby preventing further cognitive impairment or the spread of inflammation to the contralateral cortex (43).

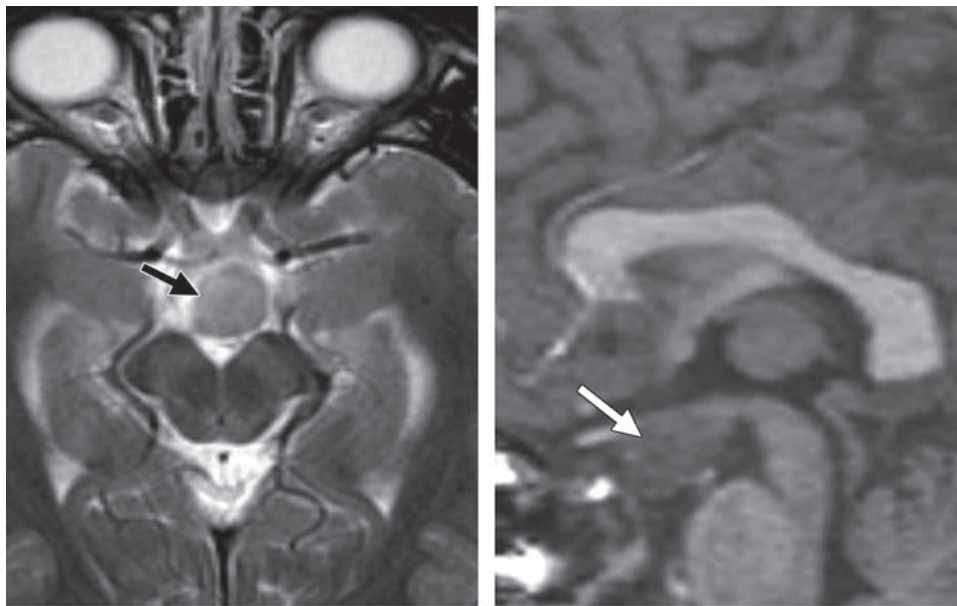


**Figure 12.** Hypothalamic hamartoma in a 7-year-old girl with gelastic seizures. **(a)** Axial T2-weighted MR image shows a slightly hyperintense hypothalamic mass (arrow). **(b)** On a sagittal contrast-enhanced T1-weighted MR image, the hypothalamic mass is unenhanced and is difficult to distinguish from the tuber cinereum (arrow).

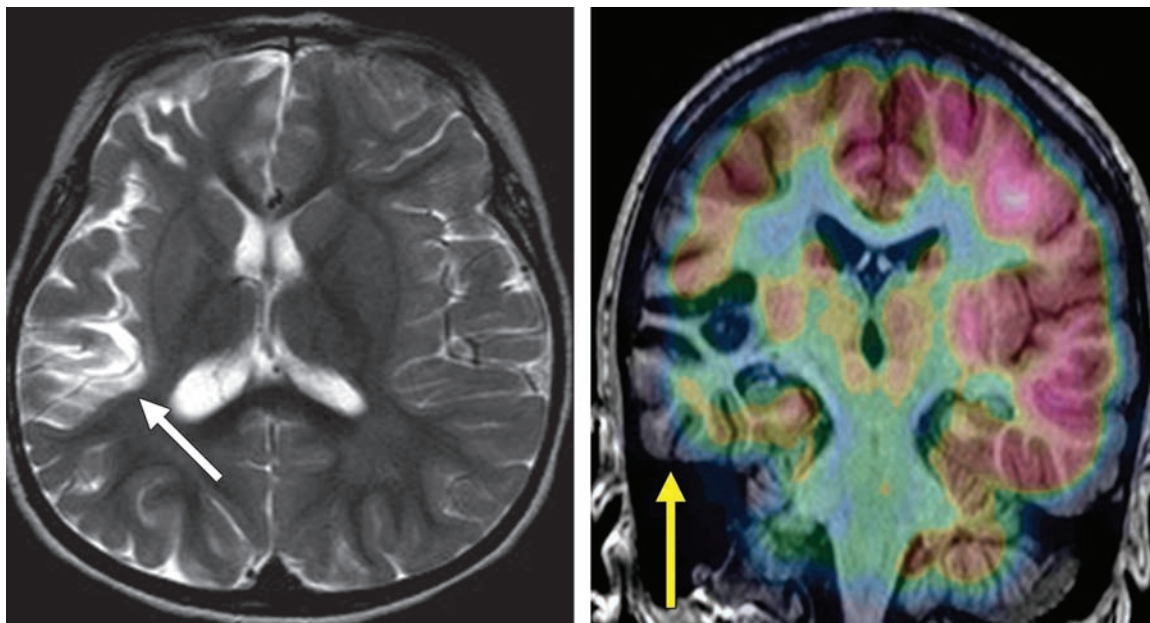


**Figure 13.** Rasmussen encephalitis in a 7-year-old child with seizures. **(a)** Axial T2-weighted MR image shows atrophy of the right temporal lobe and insular cortex that had progressed over time (arrow). **(b)** Coronal interictal MR/FDG-PET fusion image shows diffuse hypometabolic activity in the right temporal region (arrow).

Both clinical history and characteristic imaging features are necessary to make the diagnosis of Rasmussen encephalitis. The most commonly encountered imaging feature is progressive unilateral cerebral cortical atrophy (44). In the early phases of the disease, this atrophy can be seen as unilateral areas of progressive T2

hyperintensity on FLAIR images. Interictal MR/FDG-PET fusion imaging can help localize the epileptogenic foci as an area of hypometabolic activity and help identify areas of abnormality not detected at MR imaging (Fig 13) (44).

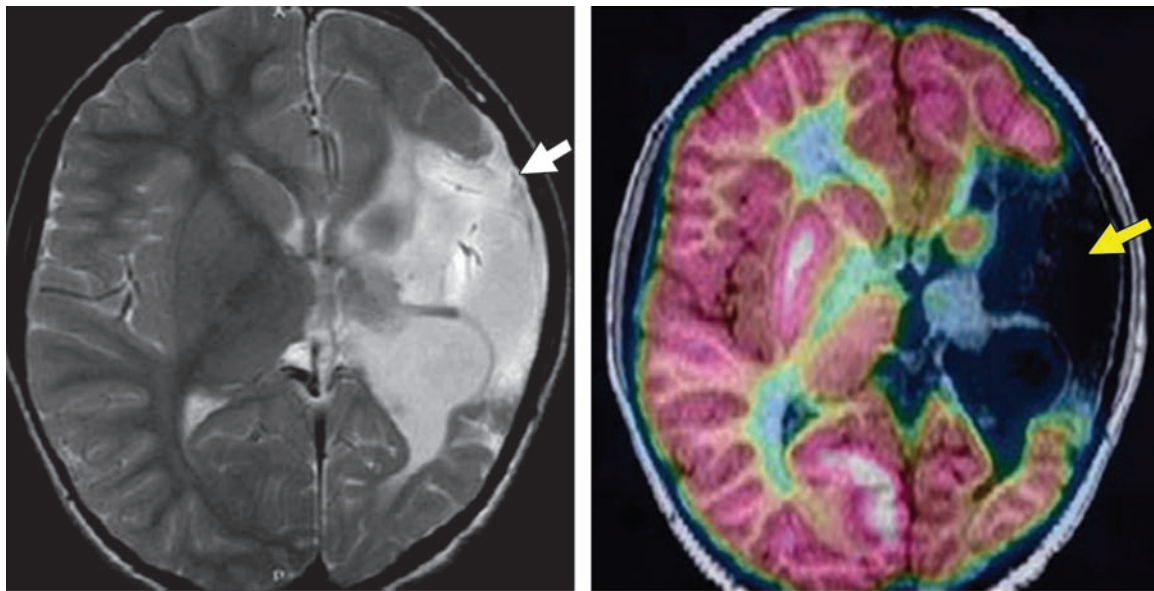


**Figure 14.** Perinatal left middle cerebral artery infarction in a 5-year-old child with seizures. **(a)** Axial T2-weighted MR image shows encephalomalacia (arrow) in the distribution of the left middle cerebral artery territory. **(b)** Axial interictal MR/FDG-PET fusion image shows hypometabolic activity (arrow) in the corresponding territory and left thalamus secondary to deafferentation.

### Perinatal Infarction

Perinatal arterial ischemic stroke refers to a cerebrovascular event occurring around the time of birth, with pathologic or radiologic evidence of focal arterial infarction (45). This diagnosis is becoming more common, likely as a result of increased detection with modern neuroimaging as well as increased clinical awareness. Its incidence (20 per 100,000 live births per year) is now estimated to equal that of large-vessel ischemic stroke in adults (46). At clinical examination, seizures in the absence of other signs of encephalopathy are often the presenting symptom. Paresis and developmental delay are other clinical features that may not be appreciated until several months after birth, resulting in a delayed diagnosis (47). The imaging features of perinatal infarction are the same as those of adult stroke and vary similarly depending on the time elapsed between the ischemic event and image acquisition (Fig 14) (45).

### Sturge-Weber Syndrome

Sturge-Weber syndrome, also known as encephalotrigeminal angiomatosis, is a rare neurocuta-

neous disorder. It is clinically characterized by epilepsy, progressive mental retardation, and facial telangiectatic nevi, often in the distribution of a trigeminal nerve division. The pathogenesis is believed to be related to a vascular steal phenomenon secondary to an extensive cortical pial angiomatous malformation. Approximately 75%–90% of patients with Sturge-Weber syndrome have epilepsy (48). Adequate pharmacologic control of epilepsy is possible in about 40% of these patients (49). Surgical treatment for medically refractory epilepsy in patients with Sturge-Weber syndrome can range from limited cortical excision to anatomic or functional hemispherectomy depending on the extent of vascular malformation (50,51).

Computed tomographic features of Sturge-Weber syndrome include (a) intracranial dense gyriform calcifications, which more commonly affect the parieto-occipital cortical areas or the choroid plexus; (b) diffuse high attenuation of the superficial and deep white matter, presumably due to microcalcifications; (c) gyriform enhancement after the administration of iodinated contrast material, reflecting pial angiomatosis; (d) brain atrophy as a consequence of vascular steal phenomena of the pial angioma on the sur-

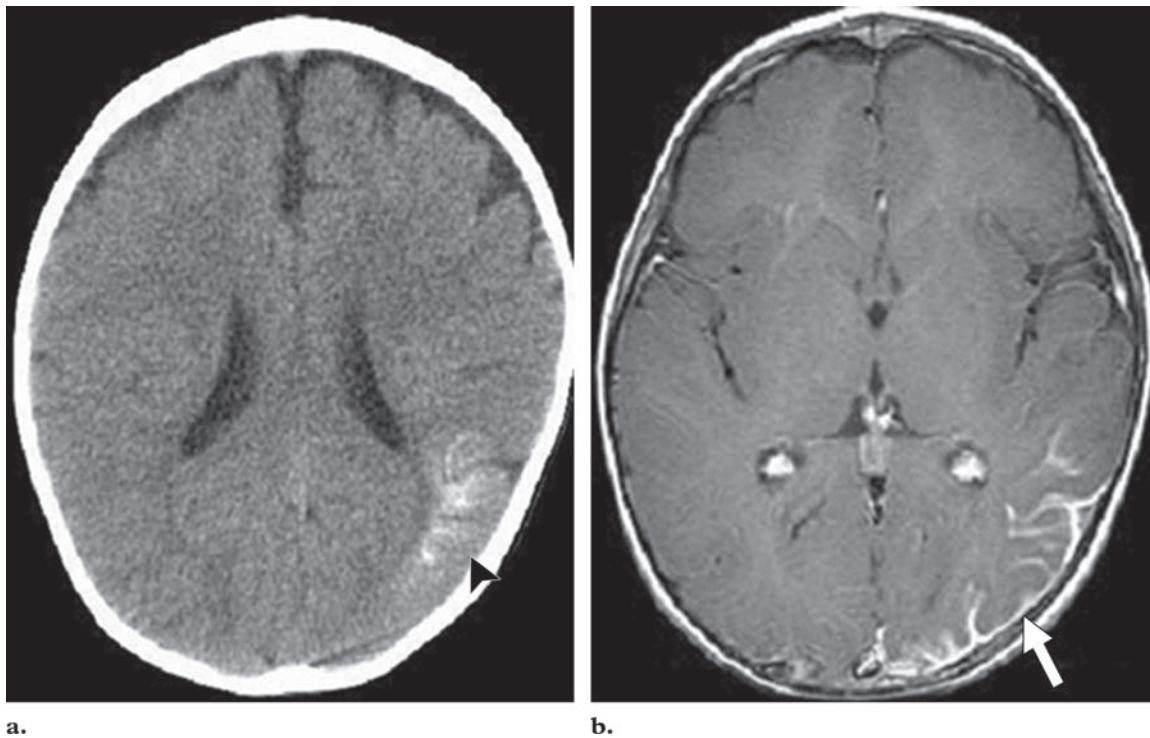


**Figure 15.** Sturge-Weber syndrome. **(a)** Unenhanced computed tomographic scan shows subcortical white matter and gray matter calcifications in the left parietal lobe (arrowhead). **(b)** Axial contrast-enhanced T1-weighted MR image shows leptomeningeal enhancement in the left temporo-occipital lobe (arrow).

rounding cortical structures; and (*e*) thickening of the calvaria as an indirect feature of loss of the brain substance (52). MR imaging is considered to be the standard of reference for the imaging of Sturge-Weber syndrome. One of the most important signs is leptomeningeal enhancement with gadolinium-based contrast agents (Fig 15) (53). On T1-weighted MR images, enlargement and abnormally avid enhancement of the ipsilateral choroid plexus may also be seen (54). T2-weighted images are used to detect areas of gliosis and cerebral atrophy likely related to chronic ischemia (52). Gradient-recalled echo images are particularly sensitive for the detection of calcifications (53).

### Conclusions

Intractable pediatric epilepsy patients represent a challenging clinical population, although advances in neuroimaging continue to improve diagnosis and treatment in these patients. Multimodality neuroimaging with MR imaging, diffusion tensor imaging, MR/FDG-PET fusion imaging, and magnetic source imaging plays an essential

role in noninvasively localizing epileptogenic foci for possible surgical resection.

### References

1. Hauser WA. The prevalence and incidence of convulsive disorders in children. *Epilepsia* 1994; 35(suppl 2):S1–S6.
2. Snead OC 3rd. Surgical treatment of medically refractory epilepsy in childhood. *Brain Dev* 2001;23: 199–207.
3. Donnelly L. *Diagnostic imaging: pediatrics*. Salt Lake City, Utah: Amirsys, 2005.
4. Sundgren PC, Dong Q, Gomez-Hassan D, Mukherji SK, Maly P, Welsh R. Diffusion tensor imaging of the brain: review of clinical applications. *Neuroradiology* 2004;46:339–350.
5. Chandra PS, Salamon N, Huang J, et al. FDG-PET/MRI coregistration and diffusion-tensor imaging distinguish epileptogenic tubers and cortex in patients with tuberous sclerosis complex: a preliminary report. *Epilepsia* 2006;47:1543–1549.
6. Juhasz C, Chugani HT. Imaging the epileptic brain with positron emission tomography. *Neuroimaging Clin N Am* 2003;13:705–716, viii.

7. Makela JP, Forss N, Jaaskelainen J, Kirveskari E, Korvenoja A, Paetau R. Magnetoencephalography in neurosurgery. *Neurosurgery* 2006;59:493–511.
8. Taylor DC, Falconer MA, Bruton CJ, Corsellis JA. Focal dysplasia of the cerebral cortex in epilepsy. *J Neurol Neurosurg Psychiatry* 1971;34:369–387.
9. Yagishita A, Arai N, Maehara T, Shimizu H, Tokumaru AM, Oda M. Focal cortical dysplasia: appearance on MR images. *Radiology* 1997;203:553–559.
10. Hudgins RJ, Flamini JR, Palasis S, Cheng R, Burns TG, Gilreath CL. Surgical treatment of epilepsy in children caused by focal cortical dysplasia. *Pediatr Neurosurg* 2005;41:70–76.
11. Tassi L, Colombo N, Garbelli R, et al. Focal cortical dysplasia: neuropathological subtypes, EEG, neuroimaging and surgical outcome. *Brain* 2002;125:1719–1732.
12. Cepeda C, Andre VM, Levine MS, et al. Epileptogenesis in pediatric cortical dysplasia: the dysmature cerebral developmental hypothesis. *Epilepsy Behav* 2006;9:219–235.
13. Palmini A, Najm I, Avanzini G, et al. Terminology and classification of the cortical dysplasias. *Neurology* 2004;62(6 suppl 3):S2–S8.
14. Vinters HV, Fisher RS, Cornford ME, et al. Morphological substrates of infantile spasms: studies based on surgically resected cerebral tissue. *Childs Nerv Syst* 1992;8:8–17.
15. Farrell MA, DeRosa MJ, Curran JG, et al. Neuropathologic findings in cortical resections (including hemispherectomies) performed for the treatment of intractable childhood epilepsy. *Acta Neuropathol (Berl)* 1992;83:246–259.
16. Palmini A, Andermann F, Olivier A, Tampieri D, Robitaille Y. Focal neuronal migration disorders and intractable partial epilepsy: results of surgical treatment. *Ann Neurol* 1991;30:750–757.
17. Kral T, Clusmann H, Blumcke I, et al. Outcome of epilepsy surgery in focal cortical dysplasia. *J Neurol Neurosurg Psychiatry* 2003;74:183–188.
18. Barkovich AJ, Raybaud CA. Neuroimaging in disorders of cortical development. *Neuroimaging Clin N Am* 2004;14:231–254, viii.
19. Osborne JP, Fryer A, Webb D. Epidemiology of tuberous sclerosis. *Ann NY Acad Sci* 1991; 615:125–127.
20. Guerreiro MM, Andermann F, Andermann E, et al. Surgical treatment of epilepsy in tuberous sclerosis: strategies and results in 18 patients. *Neurology* 1998;51:1263–1269.
21. Curatolo P. Neurological manifestations of tuberous sclerosis complex. *Childs Nerv Syst* 1996; 12:515–521.
22. Baron Y, Barkovich AJ. MR imaging of tuberous sclerosis in neonates and young infants. *AJNR Am J Neuroradiol* 1999;20:907–916.
23. Jozwiak S, Schwartz RA, Janniger CK, Bielicka-Cymerman J. Usefulness of diagnostic criteria of tuberous sclerosis complex in pediatric patients. *J Child Neurol* 2000;15:652–659.
24. Wu JY, Sutherling WW, Koh S, et al. Magnetic source imaging localizes epileptogenic zone in children with tuberous sclerosis complex. *Neurology* 2006;66:1270–1272.
25. Sims J. On the hypertrophy and atrophy of the brain. *R Med Chir Soc* 1835;19:380.
26. Di Rocco C, Battaglia D, Pietrini D, Piastra M, Massimi L. Hemimegalencephaly: clinical implications and surgical treatment. *Childs Nerv Syst* 2006;22:852–866.
27. Yagishita A, Arai N, Tamagawa K, Oda M. Hemimegalencephaly: signal changes suggesting abnormal myelination on MRI. *Neuroradiology* 1998;40:734–738.
28. Bocti C, Robitaille Y, Diadori P, et al. The pathological basis of temporal lobe epilepsy in childhood. *Neurology* 2003;60:191–195.
29. Mathern GW, Babb TL, Vickrey BG, Melendez M, Pretorius JK. The clinical-pathogenic mechanisms of hippocampal neuron loss and surgical outcomes in temporal lobe epilepsy. *Brain* 1995;118(pt 1):105–118.
30. Engel J Jr. Mesial temporal lobe epilepsy: what have we learned? *Neuroscientist* 2001;7:340–352.

31. Engel J Jr. Surgery for seizures. *N Engl J Med* 1996;334:647–652.
32. Cascino GD, Jack CR Jr, Parisi JE, et al. Magnetic resonance imaging-based volume studies in temporal lobe epilepsy: pathological correlations. *Ann Neurol* 1991;30:31–36.
33. Kuzniecky R, Jackson G. *Magnetic resonance in epilepsy*. New York, NY: Raven, 1995.
34. Knowlton RC, Laxer KD, Ende G, et al. Presurgical multimodality neuroimaging in electroencephalographic lateralized temporal lobe epilepsy. *Ann Neurol* 1997;42:829–837.
35. Raybaud C, Shroff M, Rutka JT, Chuang SH. Imaging surgical epilepsy in children. *Childs Nerv Syst* 2006;22:786–809.
36. Blumcke I, Lobach M, Wolf HK, Wiestler OD. Evidence for developmental precursor lesions in epilepsy-associated glioneuronal tumors. *Microsc Res Tech* 1999;46:53–58.
37. Koeller KK, Henry JM. From the archives of the AFIP. Superficial gliomas: radiologic-pathologic correlation. *RadioGraphics* 2001;21:1533–1556.
38. Pasquier B, Peoc HM, Fabre-Bocquentin B, et al. Surgical pathology of drug-resistant partial epilepsy: a 10-year experience with a series of 327 consecutive resections. *Epileptic Disord* 2002;4:99–119.
39. Freeman JL, Coleman LT, Wellard RM, et al. MR imaging and spectroscopic study of epileptogenic hypothalamic hamartomas: analysis of 72 cases. *AJNR Am J Neuroradiol* 2004;25:450–462.
40. Kerrigan JF, Ng YT, Prenger E, Krishnamoorthy KS, Wang NC, Rekatte HL. Hypothalamic hamartoma and infantile spasms. *Epilepsia* 2007;48:89–95.
41. Rasmussen T, Andermann F. Update on the syndrome of “chronic encephalitis” and epilepsy. *Cleve Clin J Med* 1989;56(suppl pt 2):S181–S184.
42. Bien CG, Urbach H, Deckert M, et al. Diagnosis and staging of Rasmussen’s encephalitis by serial MRI and histopathology. *Neurology* 2002;58:250–257.
43. Cook SW, Nguyen ST, Hu B, et al. Cerebral hemispherectomy in pediatric patients with epilepsy: comparison of three techniques by pathological substrate in 115 patients. *J Neurosurg* 2004;100:125–141.
44. Fiorella DJ, Provenzale JM, Coleman RE, Crain BJ, Al-Sugair AA. (18)F-fluorodeoxyglucose positron emission tomography and MR imaging findings in Rasmussen encephalitis. *AJNR Am J Neuroradiol* 2001;22:1291–1299.
45. Wu YW, Lynch JK, Nelson KB. Perinatal arterial stroke: understanding mechanisms and outcomes. *Semin Neurol* 2005;25:424–434.
46. Lee J, Croen LA, Backstrand KH, et al. Maternal and infant characteristics associated with perinatal arterial stroke in the infant. *JAMA* 2005;293:723–729.
47. Cowan F, Rutherford M, Groenendaal F, et al. Origin and timing of brain lesions in term infants with neonatal encephalopathy. *Lancet* 2003;361:736–742.
48. Di Rocco C, Tamburrini G. Sturge-Weber syndrome. *Childs Nerv Syst* 2006;22:909–921.
49. Arzimanoglou A, Aicardi J. The epilepsy of Sturge-Weber syndrome: clinical features and treatment in 23 patients. *Acta Neurol Scand Suppl* 1992;140:18–22.
50. Goscinski I, Kunicki A. On surgical treatment of Sturge-Weber syndrome. *Acta Med Pol* 1972;13:229–236.
51. Arzimanoglou AA, Andermann F, Aicardi J, et al. Sturge-Weber syndrome: indications and results of surgery in 20 patients. *Neurology* 2000;55:1472–1479.
52. Griffiths PD. Sturge-Weber syndrome revisited: the role of neuroradiology. *Neuropediatrics* 1996;27:284–294.
53. Elster AD, Chen MY. MR imaging of Sturge-Weber syndrome: role of gadopentetate dimeglumine and gradient-echo techniques. *AJNR Am J Neuroradiol* 1990;11:685–689.
54. Guermazi A, De Kerviler E, Zagdanski AM, Fria J. Diagnostic imaging of choroid plexus disease. *Clin Radiol* 2000;55:503–516.

## Neuroimaging in Pediatric Epilepsy: A Multimodality Approach

*Sachin Rastogi, MD, et al*

RadioGraphics 2008; 28:1079–1095 • Published online 10.1148/rg.284075114 • Content Codes: MR NM NR PD

---

### Page 1080

Many subtle abnormalities that may go undetected at MR imaging are more readily appreciable with fusion imaging.

### Page 1081

Magnetic source imaging, like MR/FDG-PET fusion imaging, allows the detection of many subtle abnormalities that may otherwise go undetected with conventional MR imaging.

### Page 1081

FCD is now recognized as one of the most common causes of seizures in children with intractable epilepsy, accounting for nearly 80% of all surgically treated cases in children under 3 years of age.

### Page 1082

Regardless of the underlying disease, patients in whom the lesions are visualized at preoperative MR imaging tend to have a better outcome after surgery for epilepsy than do patients in whom the lesions are not delineated with MR imaging.

### Page 1086

Interictal MR/FDG-PET fusion imaging demonstrates tubers with epileptogenic activity as regions of hypometabolic activity that are larger than the corresponding regions of signal abnormality (ie, T2 hyperintensity for patients older than 6 months) at MR imaging.